forests

MDPI

Article

Assessing the Performance of Handheld Laser Scanning for Individual Tree Mapping in an Urban Area

Jinming Yang [1,†], Wenwen Yuan [1,†], Huicui Lu [1], Yuehan Liu [2], Yongkang Wang [3], Letong Sun [1], Shimei Li [1] and Haifang Li [1,*]

[1] School of Landscape Architecture and Forestry, Qingdao Agriculture University, Qingdao 266109, China; 201401038@qau.edu.cn (J.Y.); yuanwenwen@stu.qau.edu.cn (W.Y.); huicui.lu@qau.edu.cn (H.L.)
[2] School of Forestry, Beijing Forestry University, Beijing 100083, China
[3] School of Soil and Water Conservation, Beijing Forestry University, Beijing 100083, China
* Correspondence: lihaifang@qau.edu.cn
† These authors contributed equally to this work.

Abstract: Precise individual tree or sample-based inventories derived from 3D point cloud data of mobile laser scanning can improve our comprehensive understanding of the structure, function, resilience, biodiversity, and ecosystem services of urban forests. This study assessed the performance of a handheld laser scanning system (HLS) for the extraction of tree position, diameter at breast height (DBH), and tree height (H) in an urban area. A total of 2083 trees of 13 species from 34 plots were analyzed. The results showed that the registration of tree positions using ground control points (GCPs) demonstrated high accuracy, with errors consistently below 0.4 m, except for a few instances. The extraction accuracy of DBH for all trees and individual species remained consistently high, with a total root mean square error (RMSE) of 2.06 cm (6.89%) and a bias of 0.62 cm (2.07%). Notably, broad-leaved trees outperformed coniferous trees, with RMSE and bias values of 1.86 cm (6%) and 0.76 cm (2.46%), respectively, compared to 2.54 cm (9.46%) and 0.23 cm (0.84%), respectively. The accuracy of H extraction varied significantly among different species, with R^2 values ranging from 0.65 to 0.92. Generally, both DBH and H were underestimated compared to ground measurements. Linear mixed-effects models (LMEs) were applied to evaluate factors affecting the performance of HLS with the plot as a random factor. LME analysis revealed that plant type and terrain significantly influenced the accuracy of DBH and H derived from HLS data, while other fixed factors such as plot area, tree density, and trajectory length showed no significance. With a large sample size, we concluded that the HLS demonstrated sufficient accuracy in extracting individual tree parameters in urban forests.

Keywords: LiDAR; mobile laser scanning; personal laser scanning; forest inventory; point cloud

check for updates

Citation: Yang, J.; Yuan, W.; Lu, H.; Liu, Y.; Wang, Y.; Sun, L.; Li, S.; Li, H. Assessing the Performance of Handheld Laser Scanning for Individual Tree Mapping in an Urban Area. *Forests* **2024**, *15*, 575. https://doi.org/10.3390/f15040575

Academic Editor: Mark Vanderwel

Received: 19 February 2024
Revised: 15 March 2024
Accepted: 20 March 2024
Published: 22 March 2024

Copyright: © 2024 by the authors. Licensee MDPI, Basel, Switzerland. This article is an open access article distributed under the terms and conditions of the Creative Commons Attribution (CC BY) license (https://creativecommons.org/licenses/by/4.0/).

1. Introduction

Urban forests, with their minimal spatial footprint, provide significant ecosystem services for urban residents and wildlife. These services include promoting health and social well-being, enhancing children's cognitive development and educational success rate, fostering a strong economy and providing numerous resources, mitigating the urban heat island effect, storing and sequestering carbon, offering habitat and food for animals, and managing stormwater through green infrastructure [1,2]. Precise inventories of individual trees or sample-based parameters are fundamental for achieving a comprehensive understanding of the structure, function, resilience, biodiversity, and ecosystem services of urban forests [3,4]. In traditional plot-based forest inventories, the most frequently measured individual attributes are tree species, diameter at breast height (DBH), and tree height [5,6]. These tree attributes, either individually or in combination using species-specific equations (allometric models), are employed to compute and estimate a range of characteristics at the

tree, plot, and stand levels, including basal area, volume, biomass, carbon stock, and others [7–10]. However, the diversity of urban forests, the nuanced impacts of urban trees at a small scale, and the pronounced spatial variations in urban areas create unique site-specific differences that must be taken into account to obtain highly accurate measurements [11]. To address these site-specific variations, comprehensive and high-resolution data at local scales are essential [12].

In recent decades, close-range remote sensing has undergone rapid development, fundamentally altering the landscape of in situ forest inventories [8]. Three-dimensional point cloud data obtained through light detection and ranging (LiDAR) technology are currently being utilized for the precise extraction of forest characteristics, such as individual tree position, DBH, tree height, and forest biomass [7,13–18].

Among all LiDAR sensors and platforms, the static terrestrial laser scanning (TLS) system has the highest geometric data quality at the plot level [8]. It can capture high-quality point clouds that provide detailed information at the millimeter level [19]. Over the past decade, TLS has gained global recognition as an alternative to traditional methods for forest resource surveys [20–22]. However, TLS lacks mobility and is unable to capture the complete profile of a tree from a single viewpoint. Additionally, it is well known that artificial reference targets are needed to combine multiple scans into a single point cloud in order to cover the entire area of interest [19,23]. This inconvenience in data acquisition and processing has become a major obstacle to the widespread adoption of TLS. Recent studies have explored marker-free automated registration [20,24] to enhance the applicability of TLS in forest conditions. However, the results indicated that these methods do not achieve the same level of reliability as traditional approaches using artificial reference targets.

Mobile and portable systems greatly enhance the efficiency of data collection and have the potential to be embraced as next-generation operational tools in studying forest spatial characteristics when they achieve geometric accuracy comparable to TLS systems [8]. Its platform can be a vehicle [6,25] or a person, the latter also known as personal laser scanning (PLS) [26,27] or wearable laser scanning [28]. Depending on the platform they are mounted on, PLS can be further categorized into backpack laser scanning (BPLS) [29,30] or handheld laser scanning (HLS) [4,27,31–33]. A typical PLS system comprises a LiDAR sensor, a global navigation satellite system (GNSS) receiver, and an inertial measurement unit (IMU) [18]. However, due to weak or absent GNSS signals beneath the forest canopy, there are limitations for GNSS-based PLS in positioning. The introduction of simultaneous localization and mapping (SLAM) has empowered the latest PLS systems, particularly HLS devices, with the capability to capture detailed 3D scenarios while in motion without relying on GNSS signals. By providing spatial data in a local coordinate system, SLAM software enables raw data to be quickly pre-processed and exported to various point cloud formats even on a modest laptop [4]. Thus, PLS exhibits superior mobility and higher efficiency compared to TLS. This flexibility is particularly advantageous in forest inventory in challenging terrain and structurally complex forest environments [8]. For example, ref. [27] reported that the data acquisition time with handheld PLS (10.96 min per plot) is 4.7 times faster than with multi-scan TLS (49.9 min per plot). Additionally, Bauwens et al. [32] conducted a comparison of survey time efficiency among HLS, TLS, and the conventional field method, reporting the survey coverage times per investigator of 50 m^2/min, 0.85 m^2/min, and 0.43 m^2/min, respectively. Another advantage of HLS is the reduction in occluded areas [30]. Unlike TLS, PLS uses the movement of the operator as a platform, which can minimize occlusion effects since the trajectory through the plot is equivalent to a theoretically unlimited number of scan positions [32]. However, PLS systems usually have lower angular resolutions and ranging accuracy and larger beam divergences due to the integration of less expensive laser sensors in order to reduce weight and size. Consequently, more noise points are introduced, and PLS data quality is lower compared to TLS [31,34,35].

The state of the art in HLS has exhibited time efficiency and good performance in tree mapping [26–28,30–33,36,37]. Individual tree attributes such as tree position, DBH,

and tree height are the primary focus of researchers. For example, ref. [27] investigated up to 2466 trees from 20 sample plots with different sizes distributed across various forest types, stand structures, and terrain characteristics in Austria. The root mean square error (RMSE) of the best DBH was 2.32 cm (12%), and the highest precision of relative bias was approximately 1%, which can be considered satisfactory for operational forest inventories (FI). However, to our best knowledge, ref. [27] performed the most comprehensive study with sufficient data. Most HLS studies often collect limited data at the tree or plot levels, which may lack strong statistical robustness. Recently, ref. [31] reviewed all studies involving HLS in FI. They reported promising results but stated that the limited number of conducted studies prohibits a definitive conclusion on the current suitability of HLS systems for operational FI. After an overview of the current status and advancements in close-range remote sensing for forest observations, ref. [8] also indicated that although promising results have been demonstrated, some challenges are still ahead. For practical applications in forests, additional studies with sufficient test data are needed to provide statistically reliable conclusions, including insights into the quantity, variability, and complexity of the test data. Furthermore, most of the studies [26,28,30,32,33,35] only consider a few tree species and do not account for the influence of tree species on the accuracy of LiDAR scanning.

On the other hand, previous studies related to FI have utilized several SLAM-based HLS devices: the ZEB1 [33], ZEB-REVO [28], ZEB-REVO-RT [26], and ZEB-HORIZON [27], all developed by GeoSLAM Ltd., Nottingham, UK. The launch dates for these devices were 2013, 2015, 2017, and 2019, respectively. Unlike the other devices, which incorporate the UTM-30LX sensor, the ZEB-HORIZON is equipped with the Velodyne VLP-16 laser scanner (Velodyne LiDAR, San Jose, CA, USA). The adoption of VLP-16 has significantly enhanced both the scanning range (up to 100 m) and acquisition rate (300,000 pts/s). Nonetheless, the accuracy of the range is moderate within a range of 3 cm, and the beam divergence is relatively large (3–5 mrad), both of which impact the localization uncertainty of individual points. As a low-cost sensor that may promote the popularization of laser scanning technology in FI, additional studies are needed to assess its performance in extracting forest parameters.

In this study, we introduced a new device called LiGrip H120, developed by Beijing Green Valley Technology Co., Ltd., Beijing, China, which integrates a Velodyne VLP-16 puck LiDAR (Velodyne LiDAR, San Jose, CA, USA) sensor and a HD camera. A relatively simple forest environment within a university campus, characterized by a clear understory, was selected as the study area. This choice served two purposes: first, it facilitated measurements and laser scanning; second, the campus harbors a variety of tree species, allowing for analysis of the impact of tree species on the device performance.

The main objectives of this study are to (1) obtain sufficient single-tree attributes in an urban area using an HLS system and a standardized workflow in data acquisition and parameter extraction; (2) investigate the accuracy of tree position, DBH, and tree height estimation with reference data; and (3) assess the impact of terrain, tree species, and other factors on the accuracy of tree parameter extraction.

2. Materials and Methods

2.1. Study Area and Tree Mensuration

The area selected for PLS performance assessment in this study is located on the campus of Qingdao Agricultural University (QAU), Chengyang, Qingdao, Shandong, China (Figure 1). As a coastal and mid-latitude city, Qingdao has a typical maritime climate with four distinctive seasons. The average annual temperature is 12.6 °C, with a cold winter of 0.9 °C mean temperature from December to February and a mild summer of 23.3 °C mean temperature from June to August. The average annual precipitation is about 662 mm and is mainly distributed in summer [38,39]. The Chengyang campus of QAU was established in July 2001 on agricultural lands. Therefore, nearly all of the trees on the

campus were either planted or transplanted during the last twenty years, resulting in a heterogeneous mix in terms of species, age, and height.

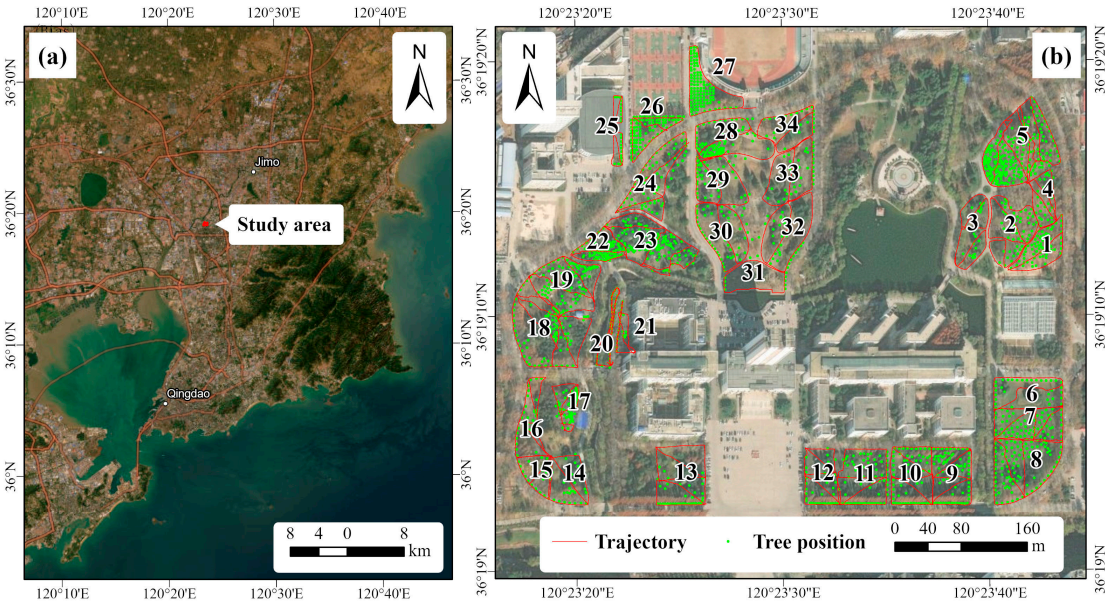

Figure 1. The location of the study area in Qingdao City, Shandong, China (**a**), and the trajectories of handheld mobile laser scanning along with the positions of trees for each plot (**b**). The numbers indicate the ID of the plots.

Different from natural forests, urban trees are dispersed across various forms of vegetated areas within built-up regions, including streets, open fields in parks, affiliated areas, or residential zones [9]. The characteristics of small forest patches and heterogeneous tree distribution determine that sample size, shape, and location greatly influence estimated parameters such as the number of trees per hectare, mean DBH, or tree height. Therefore, we selected certain green areas within the campus of QAU for our study, without specifically designing plot size. Instead, all trees with a DBH greater than 5 cm in these areas were surveyed, except for economic tree species that typically have multiple branches below 1.3 m.

The workflow of the methods executed in this study is shown in Figure 2. The tree measurements were conducted in December 2023. DBH was measured using a diameter tape with a precision of 1 mm. Tree height was primarily measured using a Blume Leiss (CGQ-1, Harbin Optical Instrument Factory Ltd., Harbin, China), which was developed to measure slope and tree height using trigonometric principles. Prior to measurement, the distance between the surveyor and the tree was ranged at 15 m or 20 m using a measuring tape, based on the estimated tree height. Then, the operator observed the treetop through the eyepiece of the device and triggered the measurement. Finally, the tree height was obtained by adding the operator's eye height to the value directly read from the device. For small trees below 10 m, height was measured directly by a tower ruler. Tree position was measured using a real-time kinematic (RTK) system (QianXun Xingyao X Plus, Qianxun SI, Shanghai, China) utilizing the projected China Geodetic Coordinate System 2000 (CGCS 2000). With real-time network calculations, the system can provide a positional accuracy of 1–3 cm.

The tree species were also recorded during the measurement work. Finally, a total of 2227 trees from 34 tree species were surveyed. However, many species had insufficient sample sizes, with some having only a single tree. To ensure robust statistical analysis, species with fewer than 20 samples were excluded. Consequently, 2083 trees from 13 species were retained. The summary information of the measured plots and the parameters of the tree species are shown in Tables 1 and 2.

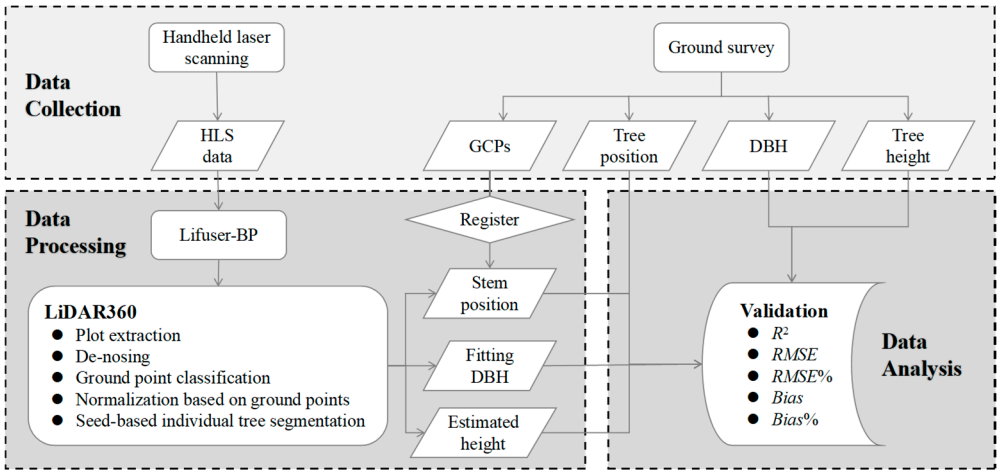

Figure 2. The workflow executed in this study.

Table 1. The summary information of the 34 measured plots on the campus of QAU (Qingdao Agricultural University).

Plot ID	*n*	DBH Range (cm)	Mean DBH (cm)	H Range (m)	Mean H (m)	Area (m^2)	Tree Density (Tree/Hectares)	Trajectory Length (m)	Scanning Time (min)	Terrain
Plot 1	67	16.1–62.9	33.7	11.2–22.7	19.1	2230	300	330	7.5	Flat
Plot 2	50	21.0–59.5	36.6	10.8–25.2	19.0	3465	144	446	11.3	Flat
Plot 3	20	10.3–41.3	21.8	5.6–14.5	9.6	2533	237	382	9.0	Flat
Plot 4	29	20.8–45.4	35.7	15.1–22.6	19.9	1566	230	335	10.1	Flat
Plot 5	259	5.1–62.5	25.2	5.0–23.7	14.4	6096	428	843	24.3	Flat
Plot 6	31	14.4–55.2	37.5	7.0–20.6	15.1	3060	101	361	9.1	Flat
Plot 7	73	11.0–57.1	22.2	6.5–21.6	9.6	3211	230	440	12.3	Flat
Plot 8	95	5.0–72.3	31.7	4.9–24.6	12.3	4995	228	475	12.6	Flat
Plot 9	69	12.7–70	33.4	8.3–23.8	16.7	3245	213	446	12.7	Flat
Plot 10	61	12.4–53.8	37.5	12.4–26.2	19.1	3444	177	446	13.1	Flat
Plot 11	66	14.3–52.7	35.5	8.4–24.0	17.6	3700	181	394	11.7	Flat
Plot 12	38	23.8–58.1	41.5	12.9–22.5	18.6	2539	161	401	12.8	Flat
Plot 13	36	12.3–63.5	43.2	8.3–23.6	19.4	4121	87	485	12.1	Flat
Plot 14	28	10.8–67.0	41.0	6.0–24.1	17.1	2443	115	287	7.2	Flat
Plot 15	19	10.3–66.5	46.6	7.7–25.6	19.5	1484	128	221	6.2	Flat
Plot 16	35	5.7–63.8	34.2	3.3–23.6	13.1	2160	204	414	9.1	Flat
Plot 17	81	5.5–43.5	18.9	3.4–18.0	12.2	936	865	237	7.4	Hilly
Plot 18	81	5.5–63.5	30.7	4.0–27.6	13.0	5943	138	611	16.8	Hilly
Plot 19	103	9.1–62.2	25.4	5.4–19.6	10.9	4865	245	557	16.5	Hilly
Plot 20	34	15.0–55.0	35.0	10.1–18.1	14.3	770	455	471	9.6	Flat
Plot 21	19	6.3–36.0	26.4	2–17.5	13.2	656	488	295	8.0	Flat
Plot 22	94	7.4–55.0	20.2	4.9–18.2	8.7	1581	626	262	7.2	Hilly
Plot 23	116	7.4–57.0	20.8	2.9–19.2	9.0	4606	280	571	17.9	Hilly
Plot 24	68	8.2–61.4	36.5	3.7–19.6	13.2	3434	198	531	14.7	Flat
Plot 25	23	9.7–18.2	14.7	6.3–8.9	7.6	808	285	303	8.6	Flat
Plot 26	95	9.1–61.2	21.2	4.9–24.6	9.0	1484	640	263	6.3	Flat
Plot 27	108	7.7–62.4	18.3	5.4–22.6	8.1	2402	450	288	5.9	Flat
Plot 28	85	5.9–62.9	28.4	4.5–21.8	11.4	3523	250	384	7.4	Flat
Plot 29	48	13.1–54.7	30.6	6.7–21.3	11.9	2880	167	312	6.5	Flat
Plot 30	50	10.0–64.0	38.0	6.1–22.4	13.8	3375	148	327	7.1	Flat
Plot 31	12	12.9–49.4	30.5	7.1–18.8	12.2	2116	57	217	5.1	Flat
Plot 32	32	13.6–72.0	42.3	8.2–21.4	16.6	3643	88	348	7.4	Flat
Plot 33	35	9.5–49.3	33.3	6.6–18.3	13.1	3211	118	326	8.5	Flat
Plot 34	23	24.9–52.7	39.3	12–18.7	15.1	2337	128	293	7.6	Flat

n is the number of trees, DBH indicates diameter at breast height, H is tree height, and mean DBH refers to the quadratic mean of DBH values.

Table 2. Summary statistics of tree species collected from 34 plots.

Plant Type	Species	*n*	DBH				Tree Height			
			Min	Max	Mean	SD	Min	Max	Mean	SD
Broadleaf	*Catalpa bungei*	47	36.4	58.1	48.3	4.9	14.6	23.1	19.2	1.7
	Fraxinus chinensis	92	15.0	57.0	31.6	7.4	9.2	20.4	14.9	2.2
	Ginkgo biloba	355	5.5	41.2	14.1	3.3	4.0	15.1	7.7	1.2
	Koelreuteria paniculata	120	5.5	38.4	21.0	6.6	3.4	19.6	12.6	3.2
	Platanus acerifolia	456	13.8	72.3	43.0	10.6	9.1	27.6	19.3	2.6
	Prunus cerasifera' Atropurpurea'	50	5.9	38.7	13.8	5.6	4.5	21.1	7.8	2.4
	Robinia pseudoacacia	49	5.1	28.5	16.3	6.1	5.0	18.0	12.4	3.1
	Salix babylonica	44	5.0	55.0	38.6	9.6	4.9	18.1	14.5	2.1
	Styphnolobium japonicum	292	5.3	70.0	26.2	11.3	3.7	23.7	13.6	3.4
	Yulania denudata	28	5.7	25.0	12.6	4.4	3.3	12.6	7.7	2.0
	Total	1533	5.0	72.3	30.9	14.7	3.3	27.6	14.1	5.2
Coniferous	*Cedrus deodara*	121	13.5	63.5	40.0	8.8	8.2	20.2	14.7	2.4
	Metasequoia glyptostroboides	125	12.3	48.4	32.3	8.4	8.3	26.2	20.0	3.4
	Pinus thunbergii	304	6.3	38.4	15.4	5.0	2.0	15.1	8.7	2.0
	Total	550	6.3	63.5	26.8	12.6	2.0	26.2	13.4	5.3

n is the number of trees, DBH indicates the diameter at breast height, mean DBH refers to the quadratic mean of DBH values, and SD indicates the standard deviation.

2.2. HLS Data Acquisition

The HLS data were collected from 6 to 9 April 2023, using the LiGrip H120 from Beijing Green Valley Technology Co., Ltd., Beijing, China (http://www.lidar360.com/archives/portfolio/ligrip-h120, accessed on 20 January 2024). This period is springtime in Qingdao, and the trees have just sprouted new leaves. The LiGrip H120 system integrates the Velodyne VLP-16 puck LiDAR sensor and a video camera with a 360° panoramic lens. The device can capture 320,000 pts/s in a single return, and the scan range is 120 m with an accuracy of ±3 cm in a field view of 280° × 360°. Based on the Simultaneous Localization and Mapping (SLAM) and Inertial Measurement Unit (IMU) techniques, the HLS system can automatically match and calibrate data reiterations. However, the performance is influenced by weather conditions (mainly wind) and obstacles from tree canopy and low shrubs.

An app installed on a smartphone or tablet is recommended for data collection. The advantage is that the operator can view current scanning data, coverage, the trajectory of the measured area, and other details in real time. The device was first placed on a stationary surface or platform without high pedestrian or vehicular traffic to complete the initialization. This process takes approximately 75 s. Subsequently, the operator held the laser device to walk through the sample plot with a stable speed of 1 m/s along the pre-designed route to collect point data and record video. Effective path planning can collect all information about the trees while reducing data redundancy. In this study, the size and shape of the measured forest area were not specified. We conducted data collection following the recommended path outlined in the equipment manual (Figure 3). If the trees are densely packed, the path would follow the Figure 3a; otherwise, Figure 3b was followed when the trees are sparse. The size of the sampled area was determined based on the requirement that the collection time does not exceed 30 min. Ensuring that the scanning path forms a closed loop significantly enhances the reliability and precision of the data. Therefore, an additional distance of 5–10 m was traveled to ensure the accurate loop closure recognized by the program.

As the device we used lacked a GNSS module, at least three ground control points (GCP) were set up along each trajectory to compare estimated tree parameters with measured results by matching absolute tree positions. During walking, the operator aligned the 'cross' hole of the marking base with each ground control point and stabilized the device to record the GCP's local coordinates in the point cloud. Once handheld marking was completed, the positions were measured using GNSS-RTK. This method is suitable

for areas with poor GNSS signals, such as dense natural forests. After all, as long as a few control points with GNSS signals are identified, it is possible to correct tree positions from the point cloud.

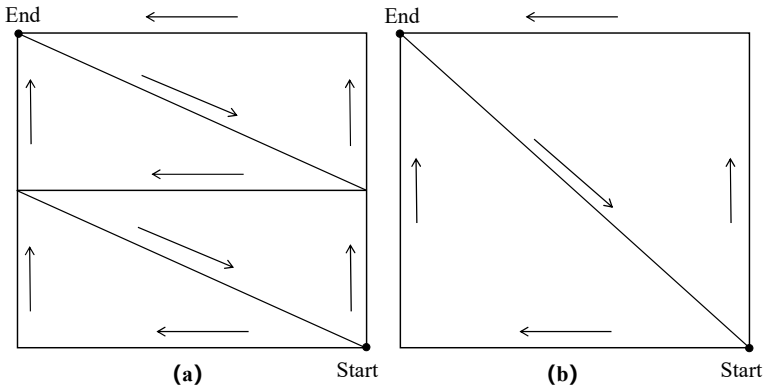

Figure 3. Path planning for dense trees (**a**) and sparse trees (**b**).

2.3. Point Cloud Processing

The raw collected data were initially fused using LiFuser-BP V1.4.2 software developed by Beijing Green Valley Technology Co., Ltd., Beijing, China. Point clouds and their corresponding trajectories were generated separately for each data acquisition from the raw data. The processed output consisted of point clouds exported in LiData files, along with the corresponding calculated trajectories and marked GCPs exported as text files. Figure 4d,e provide examples of point cloud profiles from two sample plots.

After data fusion, the LiData files and trajectories were imported into the LiDAR360 V6.0 software for further processing to extract tree parameters. Initially, the point clouds within the plots were clipped according to the trajectory lines. Subsequently, a standardized procedure with a fixed parameters setting was executed. The procedure consisted of de-noising, ground point classification, normalization based on ground points, and seed-based individual tree segmentation (Figure 2):

1. De-noising. Outliers resulting from multi-path errors or inaccuracies in the laser rangefinder during the measurement process were removed to enhance data quality. The default parameters of a neighborhood size 10 and a standard deviation multiplier 5 were adopted.
2. Ground point classification. The Improved Progressive TIN Densification (IPTD) algorithm [11] was employed for ground point classification. This algorithm initially generates a sparse triangular network using seed points and iteratively densifies it layer by layer until all ground points are classified.
3. Normalization based on ground points. The elevation value Z of the nearest ground point was subtracted from each point in the procedure of normalization to eliminate the influence of terrain undulations on the elevation values of point cloud data.
4. Seed-based individual tree segmentation. Parameters such as DBH and tree height were batch-extracted using the 'TLS Seed Point Editor' tool under 'TLS Forest', based on normalized ground points. DBH was determined by cylinder fitting within the slice at a height of 1.2–1.4 m. Subsequently, each fitted DBH and tree height was inspected for anomalies, as well as potential commission or omission errors. In case of fitting errors, individual tree fitting would be carried out again. Finally, the fitted results were used as seed points for individual tree segmentation using the 'Point Cloud Segmentation from Seed Points' tool.

The tree positions derived from the point clouds refer to the center point coordinate of the trunk at a height of 1.3 m. They were registered to the CGCS 2000 coordinate system using the affine transformation method based on GCPs to match the positions of measured trees. This process was operated through a spatial adjustment tool in the

ArcGIS 10.4 software (Environmental Systems Research Institute, Redlands, CA, USA). Figure 5 gives an example of registering the tree positions and trajectories using the affine transformation method. The scanning time for each plot was obtained from the trajectory's log file. Additionally, the trajectory files were used to calculate the trajectory length and area of each plot using the ArcGIS 10.4 software.

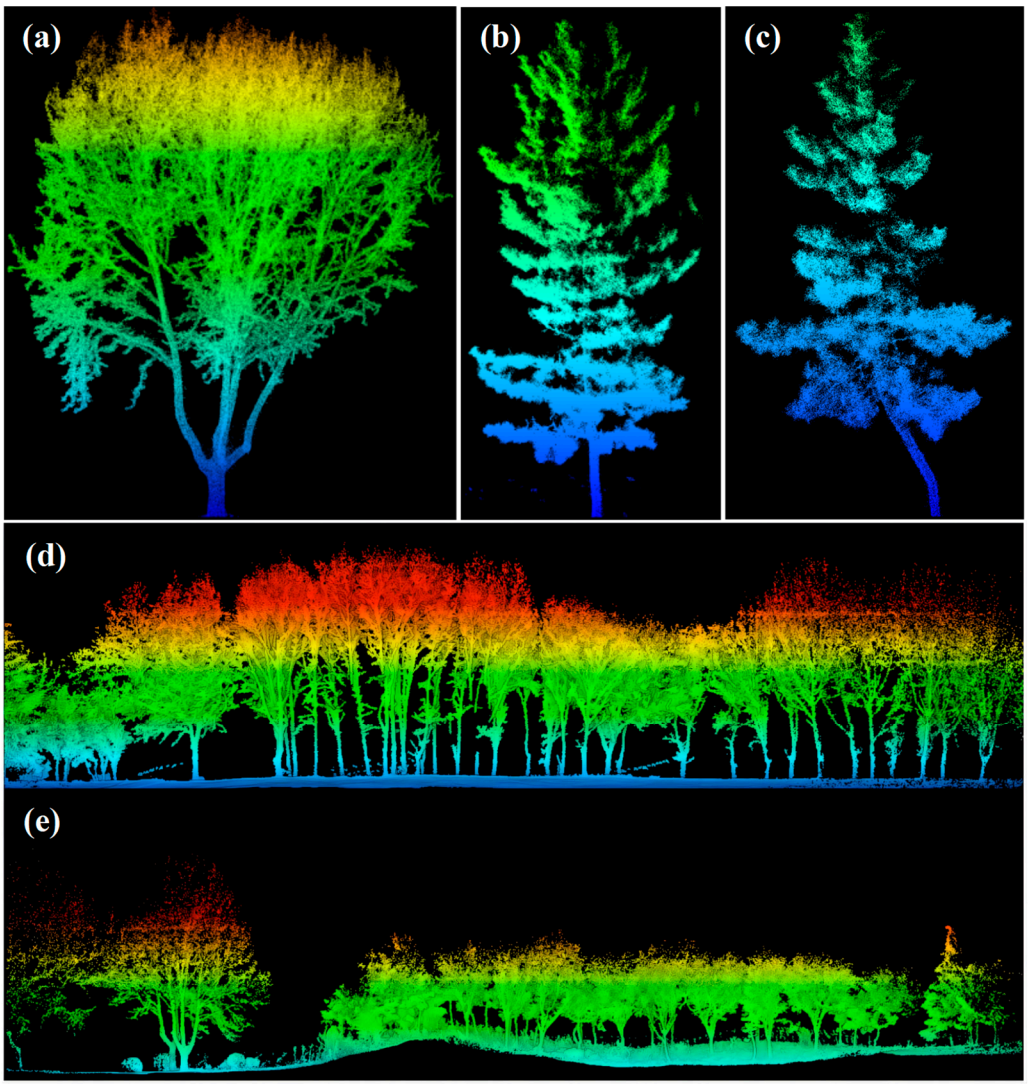

Figure 4. Point clouds of (**a**) a *Platanus acerifolia* tree, (**b**) a straight-trunked *Pinus thunbergii* tree, (**c**) a curved-trunked *Pinus thunbergii* tree, (**d**) a profile from flat ground, and (**e**) a profile from a hilly area.

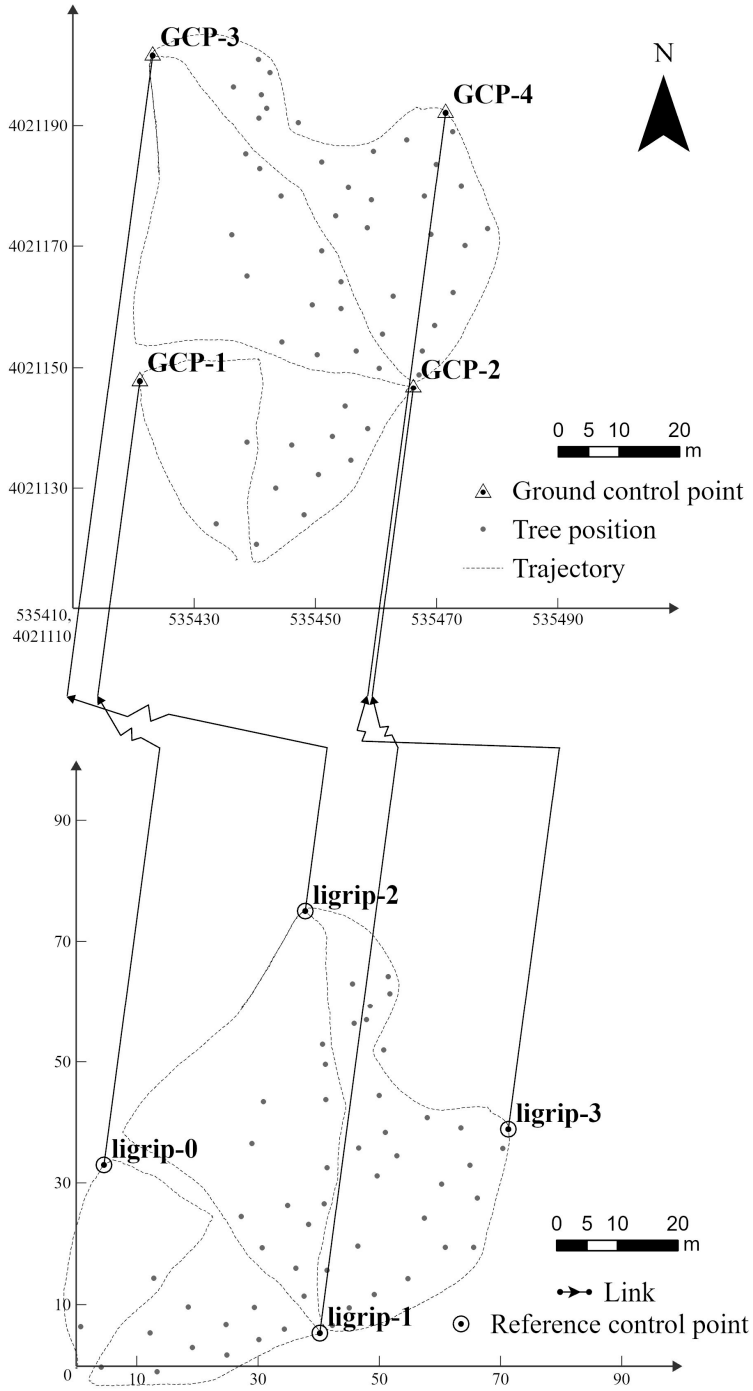

Figure 5. An example of registering tree positions and trajectory using the affine transformation method. GCP indicates the ground control point, while ligrip refers to its corresponding local coordinates marked with the HLS device in the point cloud.

2.4. Evaluation

In order to assess the accuracy of DBH and tree height derived from HLS point clouds for different species and plots, the total explained variance (R^2), root mean squared error (RMSE), relative RMSE (RMSE%), absolute bias (Bias), and relative bias (Bias%) were calculated using Equations (1)–(5):

$$R^2 = 1 - \frac{\sum_{i=1}^{n}(y_i - \hat{y}_i)^2}{\sum_{i=1}^{n}(y_i - \overline{y})^2}, \quad (1)$$

$$\text{RMSE} = \sqrt{\frac{\sum_{i=1}^{n}(y_i - \hat{y}_i)^2}{n}}, \quad (2)$$

$$\text{RMSE\%} = \frac{RMSE}{\overline{y}} \times 100\%, \quad (3)$$

$$\text{Bias} = \frac{\sum_{i=1}^{n}(y_i - \hat{y}_i)}{n}, \quad (4)$$

$$\text{Bias\%} = \frac{Bias}{\overline{y}} \times 100\%, \quad (5)$$

where n is the number of individuals of a tree species, plot, or the whole number of detected trees; y_i is the field-measured DBH or tree height of tree i; $\hat{y}_i$ indicate the estimated DBH or tree height value of tree i from HLS point clouds; and $\overline{y}$ denotes the mean DBH or tree height value of n.

2.5. Statistical Analysis

In order to assess the factors affecting the performance of HLS in tree mapping, linear mixed-effects model (LME) analysis was applied (Equation (6)).

$$\begin{aligned} Y_i = \beta_0 + \beta_1 \times \text{area} + \beta_2 \times \text{tree density} + \beta_3 \times \text{trajectory length} + \beta_4 \times \text{plant type} + \beta_5 \times \text{terrain} + \\ \beta_6 \times \text{plot} + \varepsilon_i, \end{aligned} \quad (6)$$

where Y_i is the i-th response variable of RMSE, RMSE%, Bias, or Bias% for DBH and H; area is the scanning area of each plot (m^2); tree density is the number of trees per hectare; trajectory length is the total length of trajectory for each plot (m); plant type indicates whether the tree species is coniferous or broad-leaved; terrain indicates the topography of the plot; and ε_I is the error. We considered area, tree density, trajectory length, plant type, and terrain as fixed factors and the plot as a random factor to address the repeated measurements within the plot.

The statistical analysis was conducted with R 4.2.3 [40]. The lmer() function of the lme4 package [41] was used to execute the linear mixed-effects models. We tested all linear mixed-effects models with a random intercept to assess the significance of candidate factors on HLS performance. If the interaction effects were deemed non-significant, they were excluded to simplify the statistical model. The model with the lowest Akaike's Information Criteria (AIC) was selected, and the estimated p-values were computed. The r.squaredGLMM() function of the MuMIn package [42] was used to compare the R^2 in models. The significance threshold for all tests was set at 5%.

3. Results

3.1. Tree Position

The tree positions obtained through the registration of HLS using ground control points showed high consistency with those obtained through RTK measurements, with a maximum error of 0.39 m shown in the box plot in Figure 6. Apart from some outliers, the positional accuracy of trees from different plots varies relatively little, mostly falling within the range of 0.08 to 0.2 m.

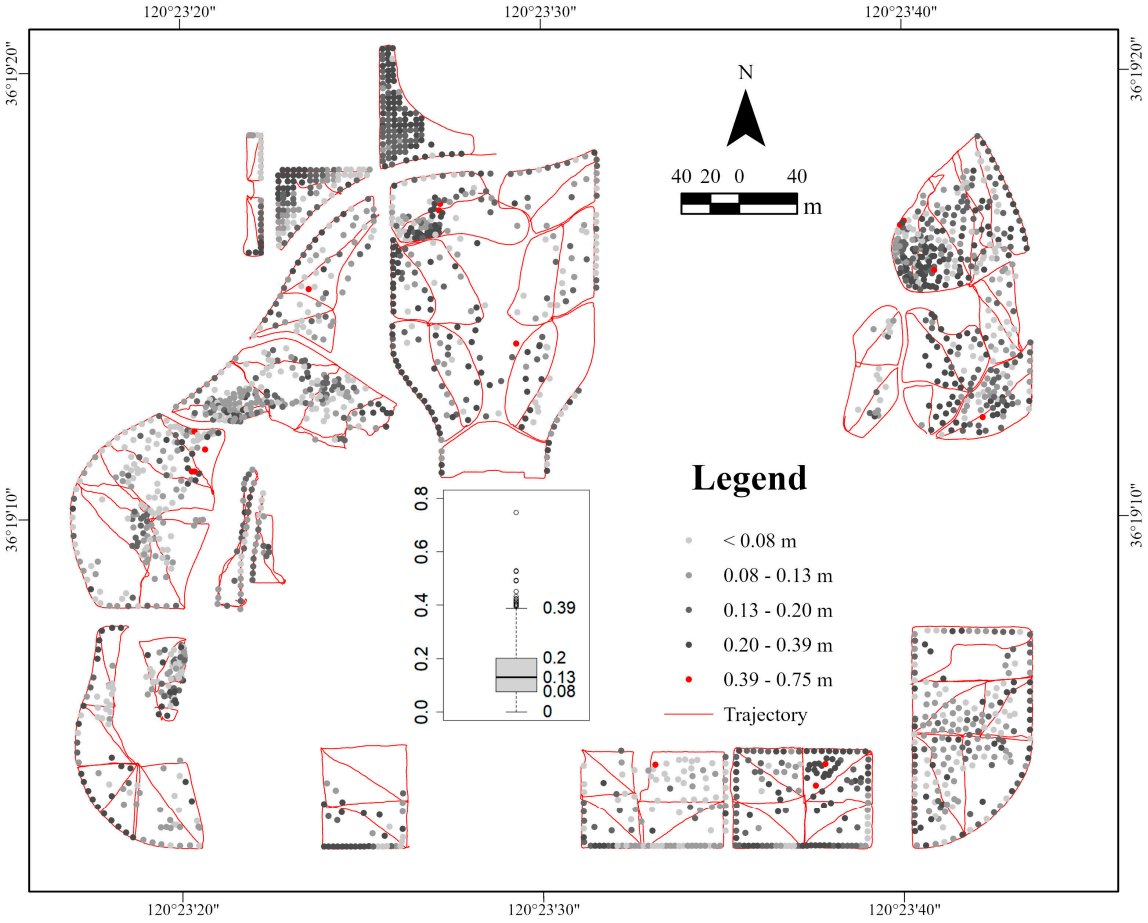

Figure 6. The accuracy of registration for tree position.

3.2. Estimation of DBH

The comparison between estimated DBH using HLS and measured DBH is shown in Figure 7. The results showed high precision, with an overall interpretive capability (R^2) of 0.98 and an RMSE of only 2.06 cm, which was about 6.89% of the quadratic mean diameter. Additionally, a slight underestimation was observed for the total of 2083 trees, with a bias of 0.62 cm (2.07%). Further analysis was conducted for coniferous and broad-leaved trees. In general, the HLS-derived DBH accuracy was better for broad-leaved trees than for coniferous trees, with the RMSE being 1.86 cm (6.01%) and 2.54 cm (9.46%), respectively. However, the bias analysis revealed that the broad-leaved trees were subject to greater underestimation compared to the coniferous trees.

For visual interpretation, specifically, 13 tree species were plotted in Figure 8. Generally, high accuracy was achieved for all tree species regarding different ranges of DBH. Except for *Pinus thunbergii*, R^2 ranged from 0.90 to 0.98. Additionally, RMSE varied between 1.26 and 2.79 cm, which was not consistent with its percent due to differences in the DBH range. Tree species with relative RMSE greater than 10% are typically those with smaller DBH. In terms of bias and relative bias, the HLS technique tended to overestimate DBH for *Koelreuteria paniculata*, *Prunus cerasifera*, *Robinia pseudoacacia*, and *Pinus thunbergii*, while it slightly underestimated other tree species. Notably, *Prunus cerasifera* exhibits a remarkably high relative bias of 7.35%. In contrast, *Koelreuteria paniculata* was one of the most accurately estimated species, with a relative bias of only 0.4%. For the majority of tree species, the relative bias falls between 1% and 5%.

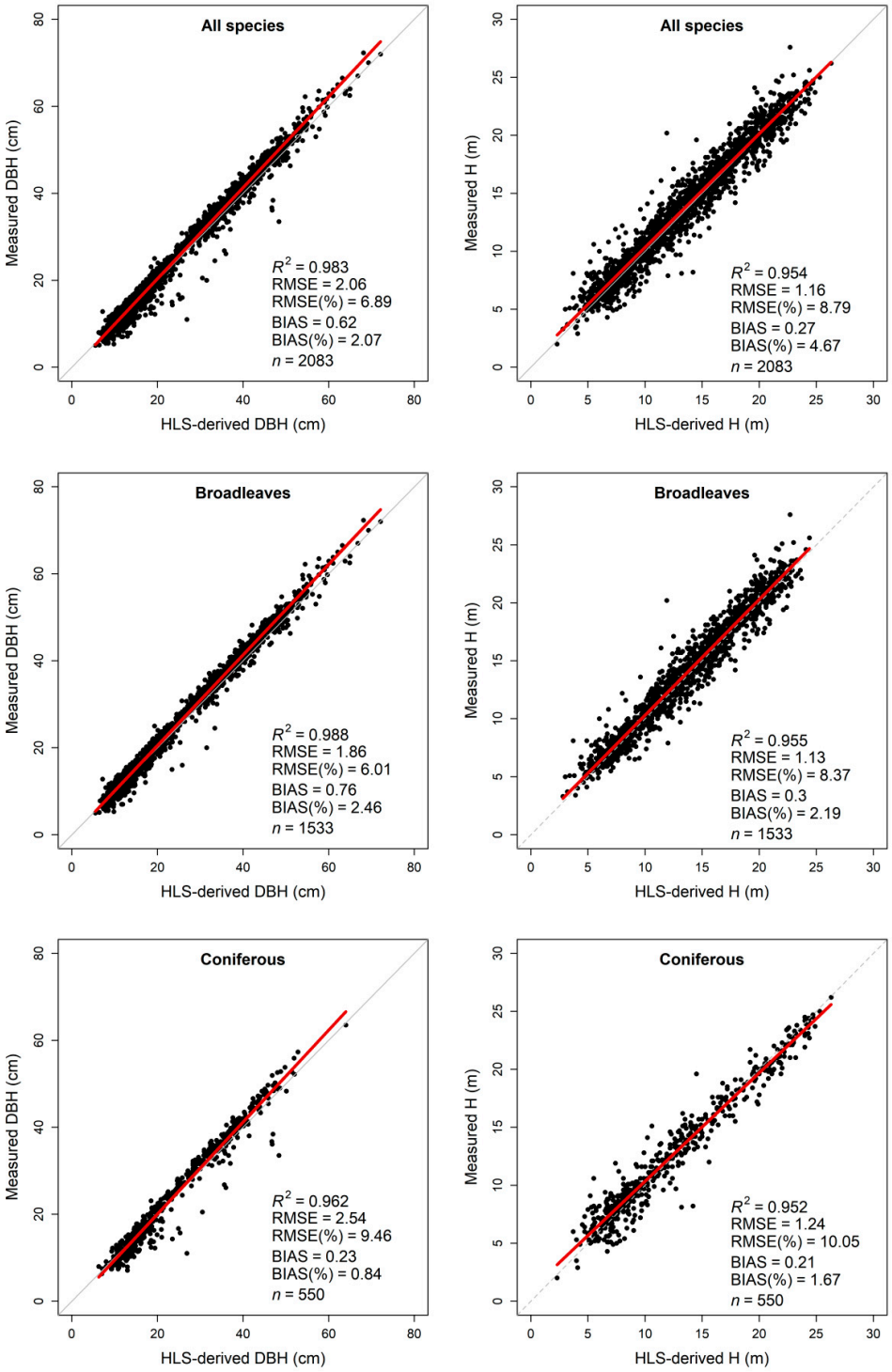

Figure 7. HLS-derived versus observed DBH (diameter at breast height) and H (tree height) for all species, broad-leaved, and coniferous trees. The red lines represent the linear regressions, while the dashed lines are the 1:1.

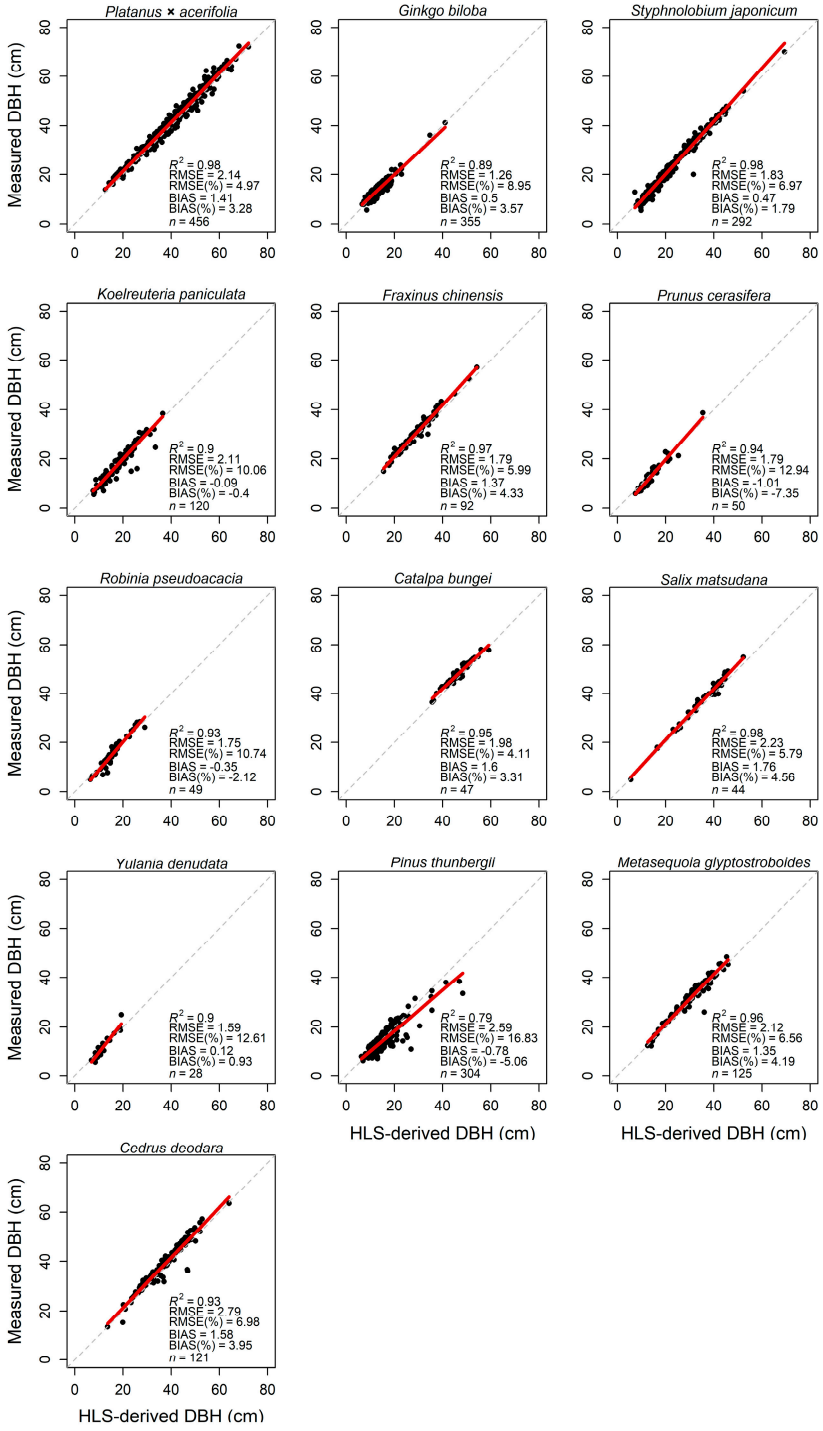

Figure 8. Comparison of the performance of HLS in estimating DBH (diameter at breast height) among 13 tree species. The red lines represent the linear regressions, while the dashed lines are the 1:1.

3.3. Estimation of Tree Height

Similar to DBH, the relationship between HLS-derived and measured tree height also resulted in a high R^2 value of 0.95 for all species of trees. As depicted in Figure 7, the RMSE reached 1.16 m, which was less than 9% of the mean height. Meanwhile, a slight underestimation in H was also observed, with a bias of 0.27 m (4.67%). Similar results were exhibited in broad-leaved and coniferous trees, with RMSE values of 1.13 m (8.37%) and 1.24 m (10.05%), respectively, and biases of 0.3 m (2.19%) and 0.21 (1.67%), respectively.

Regarding each specific tree species, the differences among them were significant (Figure 9). Firstly, the height prediction accuracy for individual tree species was much lower, ranging from a maximum of 0.92 to a minimum of 0.69, representing a 25% lower accuracy than for all trees (R^2 = 0.95). Secondly, the RMSE values ranged from 0.61 to 1.58 m, ranging from 4% to 21.4%, indicating a significant difference between species. Finally, the heights of three species (*Robinia pseudoacacia*, *Yulia deudata*, and *Metasequoia glyphostroboides*) tended to overestimate, while for other species, the trend was the opposite. These findings also suggest that the precision of DBH values was higher than that of tree height values.

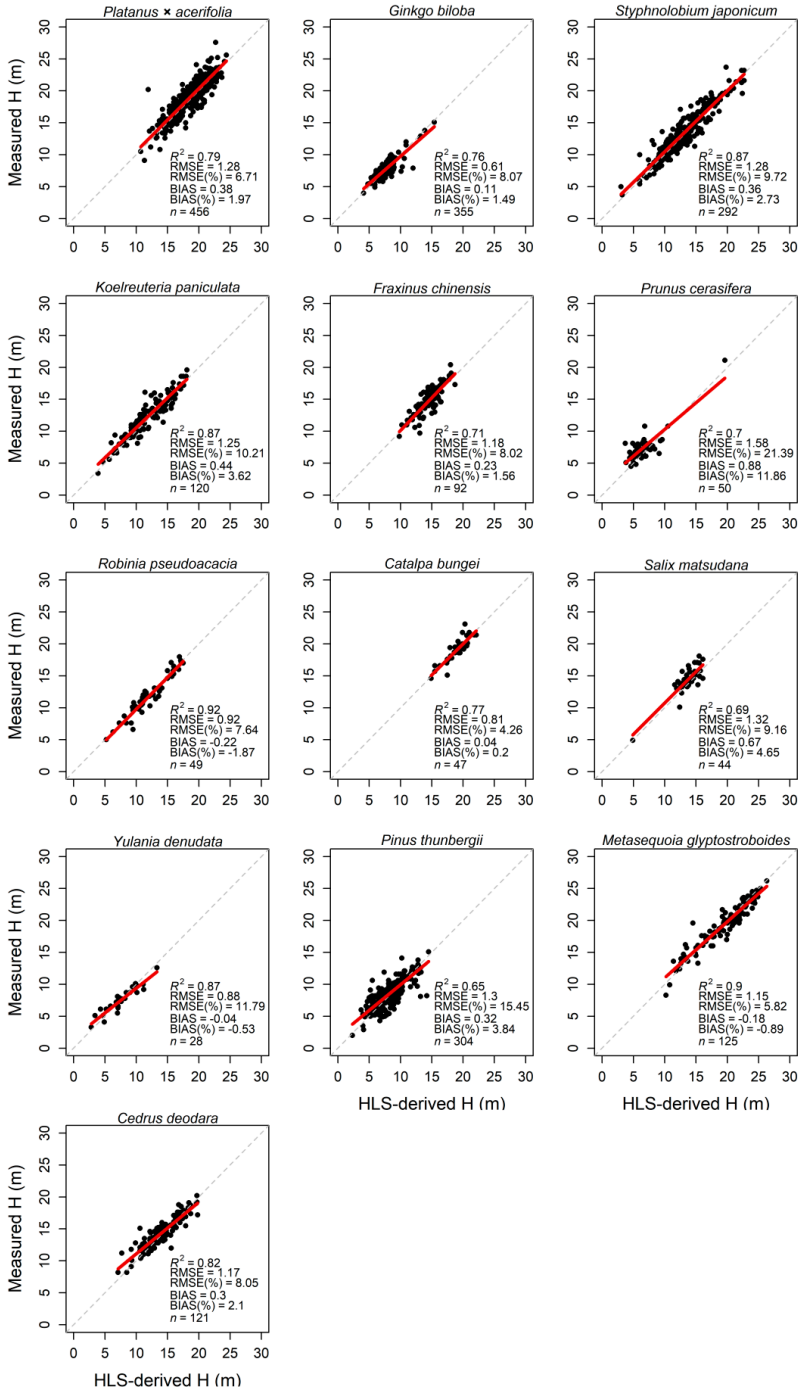

Figure 9. Comparison of the performance of HLS in estimating tree height (H) between 13 species. The red lines represent the linear regressions between measured H and HLS-derived H, while the dashed lines are the 1:1.

3.4. LME Results

In general, handheld laser scanning tends to exhibit higher accuracy in extracting DBH and tree height (H) for broad-leaved trees and trees situated in flat terrain (Figure 10). The linear mixed-effects model (LME) analysis revealed that the factors of tree density, plant type, and terrain significantly influenced the accuracy of HLS-derived DBH, whereas only the plant type significantly affected the accuracy of H (Table 3). However, in the final model, the significant influencing factors for DBH accuracy were reduced to plant type and terrain, while for accuracy of H, in addition to plant type, terrain also had a significant impact on RMSE% of H (Table 4).

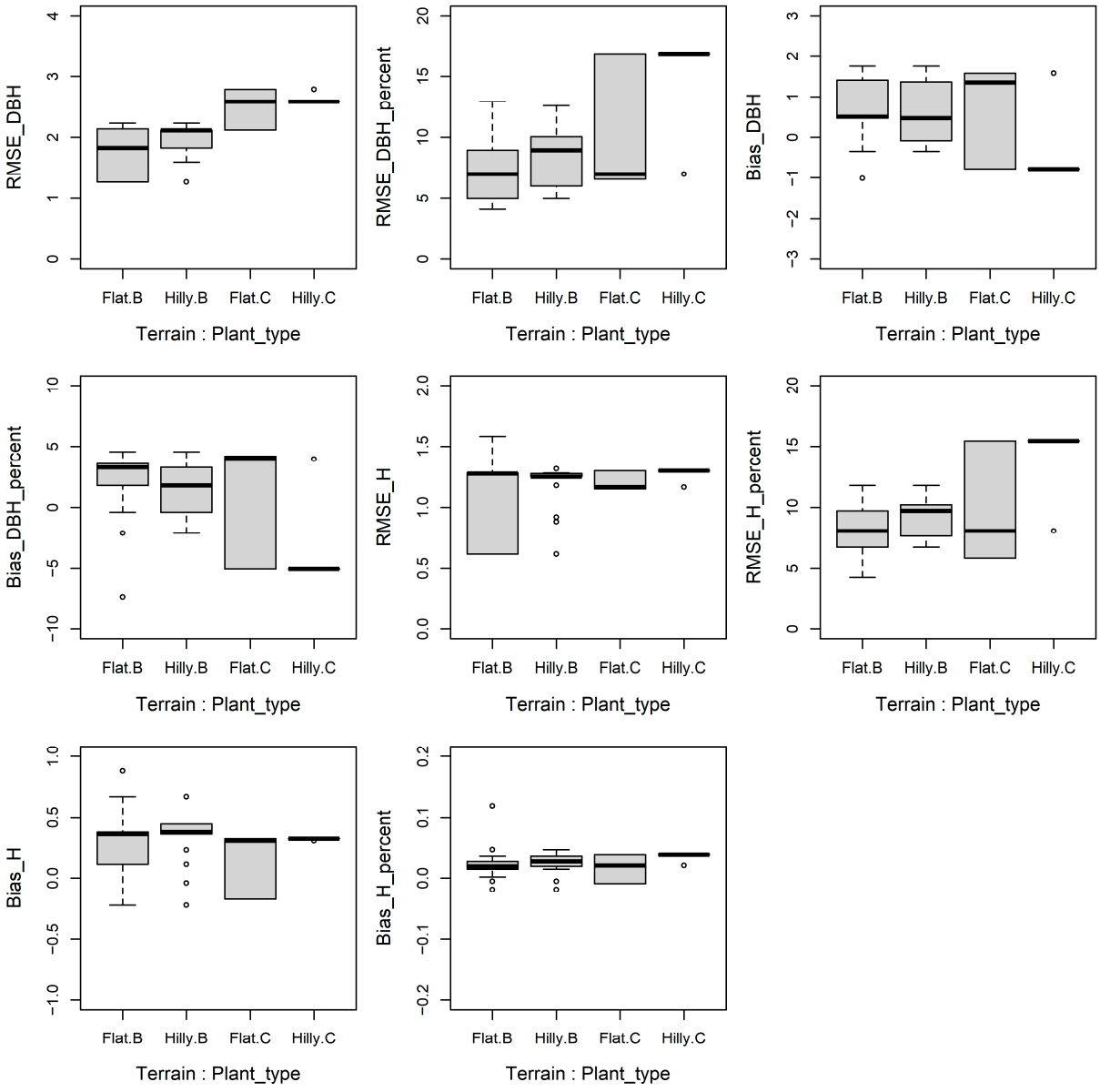

Figure 10. Boxplot illustrating the accuracy of DBH (diameter at breast height) and H (tree height) for different plant types (broad-leaved or coniferous) and terrains (flat or hilly) of the plot. Flat.B and Hilly.C denote broadleaved tree species on flat ground and conifer tree species on hilly terrain, respectively. The circular dots in the figure represent outliers.

Table 3. The coefficients (Coef.), standard errors (Std.Error), and *p*-values of linear mixed-effects models between the accuracy (RMSE, RMSE%, Bias, Bias% for DBH and H) and its candidate influence factors (tree density, trajectory length, scanning time, terrain of plot, and plant type).

Fixed Effects	**RMSE_DBH**			**RMSE%_DBH**			**Bias_DBH**			**Bias%_DBH**		
	Coef.	**Std.Error**	***p***	**Coef.**	**Std.Error**	***p***	**Coef.**	**Std.Error**	***p***	**Coef.**	**Std.Error**	***p***
Area	−0.00007	0.00005	0.2222	0.0003	0.0004	0.509	−0.0001	0.2533	0.1471	−0.0003	0.0004	0.4125
Tree density	−0.0005	0.0003	0.1188	0.0054	0.0022	0.0186	−0.0015	0.0005	0.0047	−0.0034	0.002	0.0997
Trajectory length	0.0006	0.0005	0.2230	−0.0027	0.0038	0.4916	0.0009	0.0008	0.3034	0.0016	0.0036	0.6589
Plant type/Conifer	0.6519	0.01556	$<10^{-3}$	4.9848	0.1661	$<10^{-3}$	−0.5108	0.0418	$<10^{-3}$	−2.9707	0.1521	$<10^{-3}$
Terrain/Hilly	0.2430	0.1260	0.0636	2.0013	0.9630	0.0467	−0.4746	0.2167	0.0367	−2.3887	0.8988	0.0127
Random Effects	**Variance**	**Std.Dev.**		**Variance**	**Std.Dev.**		**Variance**	**Std.Dev.**		**Variance**	**Std.Dev.**	
Plot (intercept)	0.0438	0.2094		2.516	1.5862		0.1264	0.3555		2.1942	1.4813	
Residual	0.0551	0.2348		6.3388	2.5177		0.4031	0.6349		5.3126	2.3049	
Fixed Effects	**RMSE_H**			**RMSE%_H**			**Bias_H**			**Bias%_H**		
	Coef.	**Std.Error**	***p***	**Coef.**	**Std.Error**	***p***	**Coef.**	**Std.Error**	***p***	**Coef.**	**Std.Error**	***p***
Area	−0.00004	0.00004	0.4026	0.0002	0.0005	0.7394	−0.000007	0.00003	0.8172	0.000002	0.0086	0.6041
Tree density	−0.0003	0.0002	0.1759	0.0032	0.0026	0.2201	−0.00004	0.0002	0.8138	0.00001	0.00002	0.4319
Trajectory length	0.0005	0.0004	0.2394	−0.0005	0.0045	0.9045	0.0001	0.0003	0.7024	−0.000008	0.00003	0.7829
Plant type/Conifer	0.0989	0.0111	$<10^{-3}$	3.0512	0.1603	$<10^{-3}$	−0.0799	0.0104	$<10^{-3}$	0.0026	0.001	0.0106
Terrain/Hilly	0.1655	0.1017	0.1146	1.7915	1.1351	0.1253	0.0909	0.0745	0.2327	0.0055	0.0075	0.4708
Random Effects	**Variance**	**Std.Dev.**		**Variance**	**Std.Dev.**		**Variance**	**Std.Dev.**		**Variance**	**Std.Dev.**	
Plot (intercept)	0.0286	0.1691		3.5325	1.8795		0.0153	0.1235		0.0002	0.0124	
Residual	0.0282	0.168		5.8574	2.4202		0.0248	0.1576		0.0002	0.0151	

Table 4. The coefficients (Coef.), standard errors (Std.Error), and *p*-values of final models between the accuracy (RMSE, RMSE%, Bias, Bias% for DBH and H) and its candidate influence factors (tree density, trajectory length, scanning time, terrain of plot, and plant type).

Fixed Effects	**RMSE_DBH**			**RMSE%_DBH**			**Bias_DBH**			**Bias_DBH**		
	Coef.	**Std.Error**	***p***	**Coef.**	**Std.Error**	***p***	**Coef.**	**Std.Error**	***p***	**Coef.**	**Std.Error**	***p***
Plant type/Conifer	0.6534	0.01554	$<10^{-3}$	4.9785	0.1663	$<10^{-3}$	−0.5087	0.0419	$<10^{-3}$	−2.9649	0.1521	$<10^{-3}$
Terrain/Hilly	-	-	-	3.1313	0.9009	0.0015	−0.8248	0.2074	$<10^{-3}$	−3.2282	0.7856	$<10^{-3}$
Random Effects	**Variance**	**Std.Dev.**		**Variance**	**Std.Dev.**		**Variance**	**Std.Dev.**		**Variance**	**Std.Dev.**	
Plot (intercept)	0.0453	0.2129		3.369	1.835		0.1776	0.4214		2.555	1.598	
Residual	0.0551	0.2348		6.342	2.518		0.4033	0.635		5.315	2.305	
Fixed Effects	**RMSE_H**			**RMSE%_H**			**Bias_H**			**Bias_H**		
	Coef.	**Std.Error**	***p***	**Coef.**	**Std.Error**	***p***	**Coef.**	**Std.Error**	***p***	**Coef.**	**Std.Error**	***p***
Plant type/Conifer	0.0997	0.032	$<10^{-3}$	3.0477	0.1602	$<10^{-3}$	−0.079	0.0104	$<10^{-3}$	0.0206	0.0023	0.0087
Terrain/Hilly	-	-	-	2.5277	0.9752	0.0144	-	-	-	-	-	-
Random Effects	**Variance**	**Std.Dev.**		**Variance**	**Std.Dev.**		**Variance**	**Std.Dev.**		**Variance**	**Std.Dev.**	
Plot (intercept)	0.0338	0.1839		3.971	1.993		0.0168	0.1296		0.0002	0.0131	
Residual	0.0283	0.1681		5.86	2.421		0.0249	0.1577		0.0002	0.0151	

4. Discussion

The registration of tree positions using HLS and GCPs achieved satisfactory accuracy in this study, apart from a few tilted trees, with stem positions at 1.3 m from point clouds compared to the measured base position. There are typically two approaches to obtaining absolute positions in FI by HLS. One approach is to use tightly coupled GNSS receivers and IMUs to create positioning subsystems. These subsystems capture platform movements and sensor orientation data, providing the system's position and sensor orientation at discrete

time intervals. This information enables direct georeferencing of collected data [8,43]. With a tactical-grade GNSS IMU, absolute accuracy can be reached at 0.2–0.7 m after post-processed positioning in boreal forests [25]. However, this accuracy may decrease with low-cost IMUs due to high positional drift in conditions with low GNSS visibility and increased angular uncertainty. The other approach involves registering point cloud data using GCPs, with total stations commonly used to provide high-precision coordinates [44]. These GCPs are used to georeference HLS data to the coordinate system defined by the GCPs during the registration of point clouds. Tupinambá-Simões et al. [18] compared the rigid and non-rigid modes for generating the 3D point clouds in the ZEB HLS system. Under the rigid option, the point cloud is rotated and adjusted, maintaining the scale factor, and GCP locations are matched without altering the relative positions of points. In contrast, the non-rigid mode may involve moving, rotating, or changing the scale between points, potentially altering their relative positions. They reported better performance of the non-rigid mode in the estimation of DBH. This is attributed to the use of total stations to obtain high-precision GCPs. However, setting up and using the total station is time-consuming, and it requires a known control point to initiate the measurement, which further complicates the data collection process. In our study, GCPs were not used for point cloud generating but rather for the correction of tree positions derived from point cloud post-processing. GCPs do not affect the relative positions of points, so their accuracy does not affect the extraction of DBH or tree height. Therefore, it is unnecessary to measure GCPs using a total station. We utilized real-time kinematics (RTKs) for measuring the GCPs and achieved a precise match between the stem positions in the point clouds and the measured tree positions.

In terms of DBH estimation, our study indicated high accuracy using HLS in an urban area, with RMSE ranging from 1.26 to 2.79 cm. Studies conducted in urbanized areas, including city parks, urban streets, plantation sites, and other similar environments, also demonstrated good performance in estimating DBH with HLS [26,45–47]. This was largely due to the clean and unobstructed understory within urban forests [28]. While it may seem more convenient for an operator to move through flat plots using a laser scanning device, various obstacles such as pedestrians, moving or parked cars, and landscape shrubs can still hinder the accuracy of LiDAR scanning. For instance, in a study by [48], the RMSE value of DBH for park trees was 8.95 cm, attributed to irregular trunk shapes and incomplete scanning data. In our study, factors affecting DBH accuracy mainly included inclined tree trunks, cross-section irregularities (e.g., forked, scarred, non-circular), and occlusion, which were more common in coniferous trees. The image in Figure 4c depicts an inclined tree of *Pinus thunbergii*, which decreased the fitted accuracy of DBH. As a result, broad-leaved trees exhibited higher accuracy values compared to coniferous trees. This observation aligns with findings from previous studies conducted in challenging forest environments [4,34].

Meanwhile, most previous studies were conducted with limited sample sizes, lacking sufficient robustness in their results, especially in urban areas. With a total of 2466 trees from 20 sample plots of various sizes distributed across diverse forest types, stand structures, and terrain characteristics in Austria, ref. [27] reported an RMSE of 2.32 cm (12%) in DBH, with a relative bias of approximately 1%. Our study included 2083 trees from 34 plots in an urban area, representing a sufficient sample size to evaluate the capability of HLS in extracting tree parameters. Hyyppä et al. [34] demonstrated that the RMSE for DBH derived from LiDAR data exhibited significant variability depending on the complexity of the forest plots. Consequently, more studies should be carried out in different circumstances to provide statistically reliable conclusions [8].

In comparison to DBH, tree heights were relatively inaccurate with lower R^2 and higher RMSE values, especially when considering individual tree species. Similarly, in a study by [28], tree heights were compared using a TLS and a portable laser scanner (PLS) in two plots with different tree densities in Spain. The results showed that the RMSE difference between the two devices was 1.34 m in the plot with lower density and 9.44 m in the plot with higher density. These variations were attributed to differences between the

devices and the environmental conditions of the plots. Challenging environments not only affect the performance of HLS devices but also influence the accuracy of TLS. For example, ref. [49] classified three forests into categories of Easy, Moderate, and Hard, based on tree density and vegetation cover to evaluate the accuracy of measuring tree parameters using a TLS multi-scan approach. They reported lower average accuracy compared to our study, with the RMSE and RMSE% values for height measurements ranging from 2.4 to 4.5 m and 12 to 23% for Easy conditions, and 4.0 to 7.7 m and 28 to 57% for Hard conditions.

In general, tree height was underestimated in this study, which is consistent with previous studies [34,50–52]. For instance, ref. [35] reported an underestimation of tree heights with a bias of −4.61 m and an RMSE of 2.15 m compared to field reference data using the HLS method. On the contrary, HLS tree heights were slightly overestimated in the study of [53]. However, it is essential to consider that indirect field measurements of tree height are complex [54]. Their accuracy can be influenced by various potential sources of error, such as forest structure and complexity, tree species and crown shape, leaning trees, measuring distance, tree height, instruments, and human errors. Thus, errors in tree height accuracy from HLS encompass errors associated with both HLS itself and those related to the reference field-measured tree heights.

Most of the previous studies using LiDAR for extracting tree parameters had limited sample sizes, allowing only for qualitative analysis of the impacts of forest structure, topography, etc., on the accuracy of extraction. In our study, 34 sample plots and linear mixed-effects models were employed to quantitatively analyze the effects of forest structure and other factors on the accuracy of DBH and tree height extraction. The result revealed that the plant type (broad-leaved or coniferous) and terrain were two significant factors leading to decreased accuracy of DBH and H. As stated in a study by [55], detecting spruce trees via terrestrial-based remote sensing posed considerable challenges. The dense branching and limited visibility of the lower part, especially at breast height, make it difficult for sensors to capture their entire stems. Similarly, ref. [4] analyzed the influence of stand characteristics (such as the number of trees, stand basal area, dominant height, understorey cover, slope, etc.) on HLS data accuracy using datasets from 39 sample plots. Concerning site conditions, absolute bias percentage values of arithmetic mean diameter, stand basal area, and stand volume showed a positive correlation with both ground slope and understorey cover. The errors in estimating arithmetic mean diameter and stand basal area significantly increased with understorey coverage, while errors in stand volume estimations significantly increased with slope gradient.

Finally, handheld LiDAR devices are undergoing rapid updates. During our study, a new-generation product, the LiGrip H300, part of the LiGrip handheld series from Beijing Green Valley Technology Co., Ltd., was released. Compared to its predecessor, the LiGrip H120, it boasted an increased maximum measurement range from 100 m to 300 m, a scanning frequency from 320,000 to 640,000 pts/s, and enhanced LiDAR accuracy to 1 cm. Recently, consumer-grade laser sensors have been integrated into smartphones, offering more affordable scanning technology. These affordable sensors are anticipated to proliferate in the future, offering more handheld laser scanning technology that is user-friendly [56]. Therefore, we believe that mobile and portable laser scanning systems have the potential to be embraced as next-generation operational tools.

5. Conclusions

This study evaluated the applicability of an HLS system for the examination of urban forest resource inventories and its performance in mapping individual trees. Tree position, DBH, and height were estimated by HLS from 34 different plots in QAU, and the results were compared with field measurements.

The registration of tree position using GCPs showed high accuracy with errors under 0.4 m, except for some outliers. The extraction accuracy of DBH for all trees and individual tree species was consistently high, with a total RMSE of 2.06 cm (6.89%) and a bias of 0.62 cm (2.07%). Broad-leaved trees exhibited better performance than coniferous trees,

with RMSE and bias of 1.86 cm (6%) and 0.76 cm (2.46%), respectively, compared to 2.54 cm (9.46%) and 0.23 cm (0.84%), respectively. The accuracy of tree height extraction varied significantly among different tree species in our study. The R^2 ranged from 0.65 to 0.92. Both DBH and tree height were generally underestimated. LME results revealed that plant type and terrain were the significant factors influencing the accuracy of HLS-derived DBH and tree height.

Author Contributions: Conceptualization, J.Y.; methodology, J.Y.; investigation, W.Y., Y.L., Y.W. and L.S.; data curation, W.Y. and H.L. (Huicui Lu); writing—original draft preparation, J.Y. and W.Y.; writing—review and editing, J.Y. and H.L. (Haifang Li); funding acquisition, H.L. (Huicui Lu), S.L. and H.L. (Haifang Li). All authors have read and agreed to the published version of the manuscript.

Funding: This research was funded by Qingdao Science and Technology Foundation for Public Wellbeing, grant number 23-2-8-cspz-10-nsh, National Natural Science Foundation of China, grant number 31800374, and Horizontal project of Shandong Provincial Institute of Land and Space Planning, grant numbers 6602422217 and 6602422218.

Data Availability Statement: The raw data supporting the conclusions of this article will be made available by the authors upon request.

Acknowledgments: We thank several students from Qingdao Agricultural University for data collection and compilation. The manuscript also benefited from the constructive comments and suggestions of four anonymous reviewers.

Conflicts of Interest: The authors declare no conflicts of interest.

References

1. Guo, W.; Serra-Diaz, J.; Eiserhardt, W.; Maitner, B.; Merow, C.; Violle, C.; Pound, M.; Sun, M.; Silk, F.; Blach-Overgaard, A.; et al. Climate Change and Land Use Threaten Global Hotspots of Phylogenetic Endemism for Trees. *Nat. Commun.* **2023**, *14*, 6950. [CrossRef] [PubMed]
2. Turner-Skoff, J.; Cavender, N. The Benefits of Trees for Livable and Sustainable Communities. *Plants People Planet* **2019**, *4*, 323–335. [CrossRef]
3. Derkzen, M.; van Teeffelen, A.; Verburg, P. Review: Quantifying Urban Ecosystem Services Based on High-Resolution Data of Urban Green Space: An Assessment for Rotterdam, The Netherlands. *J. Appl. Ecol.* **2015**, *52*, 1020–1032. [CrossRef]
4. Vatandaşlar, C.; Seki, M.; Zeybek, M. Assessing the Potential of Mobile Laser Scanning for Stand-Level Forest Inventories in near-Natural Forests. *For. Int. J. For. Res.* **2023**, *96*, 448–464. [CrossRef]
5. Vatandaşlar, C.; Zeybek, M. Application of Handheld Laser Scanning Technology for Forest Inventory Purposes in the NE Turkey. *Turk. J. Agric. For.* **2020**, *44*, 229–242. [CrossRef]
6. Liu, J.; Feng, Z.; Yang, L.; Mannan, A.; Khan, T.; Zhao, Z.; Cheng, Z. Extraction of Sample Plot Parameters from 3d Point Cloud Reconstruction Based on Combined RTK and CCD Continuous Photography. *Remote Sens.* **2018**, *10*, 1299. [CrossRef]
7. Brede, B.; Terryn, L.; Barbier, N.; Bartholomeus, H.; Bartolo, R.; Calders, K.; Derroire, G.; Krishna Moorthy, S.; Lau, A.; Levick, S.; et al. Non-Destructive Estimation of Individual Tree Biomass: Allometric Models, Terrestrial and Uav Laser Scanning. *Remote Sens. Environ.* **2022**, *280*, 113180. [CrossRef]
8. Liang, X.; Kukko, A.; Balenovic, I.; Saarinen, N.; Junttila, S.; Kankare, V.; Holopainen, M.; Mokros, M.; Surovy, P.; Kaartinen, H.; et al. Close-Range Remote Sensing of Forests: The State of the Art, Challenges, and Opportunities for Systems and Data Acquisitions. *IEEE Geosci. Remote Sens. Mag.* **2022**, *10*, 32–71. [CrossRef]
9. Schick, M.; Griffin, R.; Cherrington, E.; Sever, T. Utilizing Lidar to Quantify Aboveground Tree Biomass within an Urban University. *Urban For. Urban Green.* **2023**, *89*, 128098. [CrossRef]
10. Yang, J.; Zhang, M.; Zhang, J.; Lu, H.; Richard, J. Allometric Growth of Common Urban Tree Species in Qingdao City of Eastern China. *Forests* **2023**, *14*, 472. [CrossRef]
11. Zhao, C.; Sander, H. Assessing the Sensitivity of Urban Ecosystem Service Maps to Input Spatial Data Resolution and Method Choice. *Landsc. Urban Plan.* **2018**, *175*, 11–22. [CrossRef]
12. Brzoska, P.; Spāģe, A. From City- to Site-Dimension: Assessing the Urban Ecosystem Services of Different Types of Green Infrastructure. *Land* **2020**, *9*, 150. [CrossRef]
13. Brede, B.; Calders, K.; Lau, A.; Raumonen, P.; Bartholomeus, H.; Herold, M.; Kooistra, L. Non-Destructive Tree Volume Estimation through Quantitative Structure Modelling: Comparing UAV Laser Scanning with Terrestrial LiDAR. *Remote Sens. Environ.* **2019**, *233*, 111355. [CrossRef]
14. Kuželka, K.; Marušák, R.; Surový, P. Inventory of Close-to-Nature Forest Stands Using Terrestrial Mobile Laser Scanning. *Int. J. Appl. Earth Obs. Geoinf.* **2022**, *115*, 103104. [CrossRef]

15. Liang, X.; Wang, Y.; Jaakkola, A.; Kukko, A.; Kaartinen, H.; Hyyppa, J.; Honkavaara, E.; Liu, J. Forest Data Collection Using Terrestrial Image-Based Point Clouds from a Handheld Camera Compared to Terrestrial and Personal Laser Scanning. *IEEE Trans. Geosci. Remote Sens.* **2015**, *53*, 5117–5132. [CrossRef]
16. Münzinger, M.; Prechtel, N.; Behnisch, M. Mapping the Urban Forest in Detail: From LiDAR Point Clouds to 3D Tree Models. *Urban. For. Urban Green.* **2022**, *74*, 127637. [CrossRef]
17. Su, Y.; Guo, Q.; Xue, B.; Hu, T.; Alvarez, O.; Tao, S.; Fang, J. Spatial Distribution of Forest Aboveground Biomass in China: Estimation through Combination of Spaceborne Lidar, Optical Imagery, and Forest Inventory Data. *Remote Sens. Environ.* **2016**, *173*, 187–199. [CrossRef]
18. Tupinambá-Simões, F.; Pascual, A.; Guerra-Hernández, J.; Ordóñez, C.; de Conto, T.; Bravo, F. Assessing the Performance of a Handheld Laser Scanning System for Individual Tree Mapping—A Mixed Forests Showcase in Spain. *Remote Sens.* **2023**, *15*, 1169. [CrossRef]
19. Liang, X.; Kankare, V.; Hyyppä, J.; Wang, Y.; Kukko, A.; Haggrén, H.; Yu, X.; Kaartinen, H.; Jaakkola, A.; Guan, F.; et al. Terrestrial Laser Scanning in Forest Inventories. *ISPRS J. Photogramm Remote Sens.* **2016**, *115*, 63–77. [CrossRef]
20. Guan, H.; Su, Y.; Sun, X.; Xu, G.; Li, W.; Ma, Q.; Wu, X.; Wu, J.; Liu, L.; Guo, Q. A Marker-Free Method for Registering Multi-Scan Terrestrial Laser Scanning Data in Forest Environments. *ISPRS J. Photogramm. Remote Sens.* **2020**, *166*, 82–94. [CrossRef]
21. Moskal, L.; Zheng, G. Retrieving Forest Inventory Variables with Terrestrial Laser Scanning (TLS) in Urban Heterogeneous Forest. *Remote Sens.* **2011**, *4*, 1–20. [CrossRef]
22. Watt, P.; Donoghue, D. Measuring Forest Structure with Terrestrial Laser Scanning. *Int. J. Remote Sens.* **2005**, *26*, 1437–1446. [CrossRef]
23. Wilkes, P.; Lau, A.; Disney, M.; Calders, K.; Burt, A.; Gonzalez de Tanago, J.; Bartholomeus, H.; Brede, B.; Herold, M. Data Acquisition Considerations for Terrestrial Laser Scanning of Forest Plots. *Remote Sens. Environ.* **2017**, *196*, 140–153. [CrossRef]
24. Tremblay, J.; Béland, M. Towards Operational Marker-free Registration of Terrestrial Lidar Data in Forests. *ISPRS J. Photogramm Remote Sens.* **2018**, *146*, 430–435. [CrossRef]
25. Kukko, A.; Kaijaluoto, R.; Kaartinen, H.; Lehtola, V.; Jaakkola, A.; Hyyppä, J. Graph Slam Correction for Single Scanner MLS Forest Data under Boreal Forest Canopy. *ISPRS J. Photogramm Remote Sens.* **2017**, *132*, 199–209. [CrossRef]
26. Chen, S.; Liu, H.; Feng, Z.; Shen, C.; Chen, P. Applicability of Personal Laser Scanning in Forestry Inventory. *PLoS ONE* **2019**, *14*, e0211392. [CrossRef]
27. Gollob, C.; Ritter, T.; Nothdurft, A. Forest Inventory with Long Range and High-Speed Personal Laser Scanning (PLS) and Simultaneous Localization and Mapping (Slam) Technology. *Remote Sens.* **2020**, *12*, 1509. [CrossRef]
28. Cabo, C.; Del Pozo, S.; Rodríguez-Gonzálvez, P.; Ordóñez, C.; González-Aguilera, D. Comparing Terrestrial Laser Scanning (TLS) and Wearable Laser Scanning (WLS) for Individual Tree Modeling at Plot Level. *Remote Sens.* **2018**, *10*, 540. [CrossRef]
29. Liu, L.; Zhang, A.; Xiao, S.; Hu, S.; He, N.; Pang, H.; Zhang, X.; Yang, S. Single Tree Segmentation and Diameter at Breast Height Estimation with Mobile LiDAR. *IEEE Access* **2021**, *9*, 24314–24325. [CrossRef]
30. Oveland, I.; Hauglin, M.; Giannetti, F.; Kjørsvik, N.; Gobakken, T. Comparing Three Different Ground Based Laser Scanning Methods for Tree Stem Detection. *Remote Sens.* **2018**, *10*, 538. [CrossRef]
31. Balenovic, I.; Liang, X.; Jurjevic, L.; Hyyppä, J.; Seletković, A.; Kukko, A. Hand-Held Personal Laser Scanning. *Croat. J. For. Eng.* **2021**, *42*, 165–183. [CrossRef]
32. Bauwens, S.; Bartholomeus, H.; Calders, K.; Lejeune, P. Forest Inventory with Terrestrial LiDAR: A Comparison of Static and Hand-Held Mobile Laser Scanning. *Forests* **2016**, *7*, 127. [CrossRef]
33. Ryding, J.; Williams, E.; Smith, M.; Eichhorn, M. Assessing Handheld Mobile Laser Scanners for Forest Surveys. *Remote Sens.* **2015**, *7*, 1095–1111. [CrossRef]
34. Hyyppä, E.; Yu, X.; Kaartinen, H.; Hakala, T.; Kukko, A.; Vastaranta, M.; Hyyppä, J. Comparison of Backpack, Handheld, under-Canopy UAV, and above-Canopy UAV Laser Scanning for Field Reference Data Collection in Boreal Forests. *Remote Sens.* **2020**, *12*, 3327. [CrossRef]
35. Giannetti, F.; Puletti, N.; Quatrini, V.; Travaglini, D.; Bottalico, F.; Corona, P.; Chirici, G. Integrating terrestrial and airborne laser scanning for the assessment of single-tree attributes in Mediterranean forest stands. *Eur. J. Remote Sens.* **2018**, *51*, 795–807. [CrossRef]
36. Proudman, A.; Ramezani, M.; Digumarti, S.; Chebrolu, N.; Fallon, M. Towards real-time forest inventory using handheld LiDAR. *Robot. Auton. Syst.* **2022**, *157*, 104240. [CrossRef]
37. Winberg, O.; Pyörälä, J.; Yu, X.; Kaartinen, H.; Kukko, A.; Holopainen, M.; Holmgren, J.; Lehtomäki, M.; Hyyppä, J. Branch information extraction from Norway spruce using handheld laser scanning point clouds in Nordic forests. *ISPRS Open J. Photogramm. Remote Sens.* **2023**, *9*, 100040. [CrossRef]
38. Yang, J.; Li, X.; Li, S.; Liang, H.; Lu, H. The Woody Plant Diversity and Landscape Pattern of Fine-Resolution Urban Forest Along a Distance Gradient from Points of Interest in Qingdao. *Ecol. Indic.* **2021**, *122*, 107326. [CrossRef]
39. Yang, J.; Li, S.; Lu, H. Quantitative Influence of Land-Use Changes and Urban Expansion Intensity on Landscape Pattern in Qingdao, China: Implications for Urban Sustainability. *Sustainability* **2019**, *11*, 6174. [CrossRef]
40. R Core Team. *R: A Language and Environment for Statistical Computing*; R Foundation for Statistical Computing: Vienna, Austria, 2018; Available online: https://www.R-project.org/ (accessed on 25 January 2024).

41. Bates, D.; Maechler, M.; Bolker, B.; Walker, S. Lme4: Mixed-Effects Models in R. 2013. Available online: https://github.com/lme4/lme4/ (accessed on 25 January 2024).
42. Barton, K. Mumin: Multi-Model Inference. R Package Version 1.47.5. 2013. Available online: http://cran.r-project.org/package=MuMIn (accessed on 25 January 2024).
43. Puente, I.; González-Jorge, H.; Martínez-Sánchez, J.; Arias, P. Review of Mobile Mapping and Surveying Technologies. *Measurement* **2013**, *46*, 2127–2145. [CrossRef]
44. Piermattei, L.; Karel, W.; Wang, D.; Wieser, M.; Mokroš, M.; Surový, P.; Koreň, M.; Tomaštík, J.; Pfeifer, N.; Hollaus, M. Terrestrial Structure from Motion Photogrammetry for Deriving Forest Inventory Data. *Remote Sens.* **2019**, *11*, 950. [CrossRef]
45. Guo, Q.; Su, Y.; Hu, T.; Guan, H.; Jin, S.; Zhang, J.; Zhao, X.; Xu, K.; Wei, D.; Kelly, M.; et al. Lidar Boosts 3D Ecological Observations and Modelings: A Review and Perspective. *IEEE Geosci. Remote Sens. Mag.* **2021**, *9*, 232–257. [CrossRef]
46. Jurjević, L.; Liang, X.; Gašparović, M.; Balenović, I. Is Field-Measured Tree Height as Reliable as Believed—Part II, a Comparison Study of Tree Height Estimates from Conventional Field Measurement and Low-Cost Close-Range Remote Sensing in a Deciduous Forest. *ISPRS J. Photogramm. Remote Sens.* **2020**, *169*, 227–241. [CrossRef]
47. Zhou, S.; Kang, F.; Li, W.; Kan, J.; Zheng, Y.; He, G. Extracting Diameter at Breast Height with a Handheld Mobile LiDAR System in an Outdoor Environment. *Sensors* **2019**, *19*, 3212. [CrossRef] [PubMed]
48. Heo, H.; Lee, D.; Park, J.; Thorne, J. Estimating the Heights and Diameters at Breast Height of Trees in an Urban Park and Along a Street Using Mobile LiDAR. *Landsc. Ecol. Eng.* **2019**, *15*, 253–263. [CrossRef]
49. Liang, X.; Hyyppä, J.; Kaartinen, H.; Lehtomäki, M.; Pyörälä, J.; Pfeifer, N.; Holopainen, M.; Brolly, G.; Francesco, P.; Hackenberg, J.; et al. International Benchmarking of Terrestrial Laser Scanning Approaches for Forest Inventories. *ISPRS J. Photogramm. Remote Sens.* **2018**, *144*, 137–179. [CrossRef]
50. Sofia, S.; Maetzke, F.; Crescimanno, M.; Coticchio, A.; La Mela Veca, D.; Galati, A. The Efficiency of Lidar Hmls Scanning in Monitoring Forest Structure Parameters: Implications for Sustainable Forest Management. *Eur. Med. J. Bus.* **2022**, *17*, 350–373. [CrossRef]
51. Chiappini, S.; Pierdicca, R.; Malandra, F.; Tonelli, E.; Malinverni, E.; Urbinati, C.; Vitali, A. Comparing Mobile Laser Scanner and Manual Measurements for Dendrometric Variables Estimation in a Black Pine (*Pinus nigra* Arn.) Plantation. *Comput. Electron. Agric.* **2022**, *198*, 107069. [CrossRef]
52. Donager, J.; Sánchez Meador, A.; Blackburn, R. Adjudicating Perspectives on Forest Structure: How Do Airborne, Terrestrial, and Mobile Lidar-Derived Estimates Compare? *Remote Sens.* **2021**, *13*, 2297. [CrossRef]
53. Jurjević, L.; Gašparović, M.; Liang, X.; Balenović, I. Assessment of Close-Range Remote Sensing Methods for DTM Estimation in a Lowland Deciduous Forest. *Remote Sens.* **2021**, *13*, 2063. [CrossRef]
54. Persson, H.; Olofsson, K.; Holmgren, J. Two-Phase Forest Inventory Using Very-High-Resolution Laser Scanning. *Remote Sens. Environ.* **2022**, *271*, 112909. [CrossRef]
55. Liang, X.; Wang, Y.; Pyörälä, J.; Lehtomäki, M.; Yu, X.; Kaartinen, H.; Kukko, A.; Honkavaara, E.; Issaoui, A.; Nevalainen, O.; et al. Forest in Situ Observations Using Unmanned Aerial Vehicle as an Alternative of Terrestrial Measurements. *Forest Ecosyst.* **2019**, *6*, 20. [CrossRef]
56. Mokroš, M.; Mikita, T.; Singh, A.; Tomaštík, J.; Chudá, J.; Wężyk, P.; Kuželka, K.; Surový, P.; Klimánek, M.; Zięba-Kulawik, K.; et al. Novel Low-Cost Mobile Mapping Systems for Forest Inventories as Terrestrial Laser Scanning Alternatives. *Int. J. Appl. Earth Obs. Geoinf.* **2021**, *104*, 102512. [CrossRef]

Disclaimer/Publisher's Note: The statements, opinions and data contained in all publications are solely those of the individual author(s) and contributor(s) and not of MDPI and/or the editor(s). MDPI and/or the editor(s) disclaim responsibility for any injury to people or property resulting from any ideas, methods, instructions or products referred to in the content.